



Published in final edited form as:

Retina. 2013 October ; 33(9): 1850–1862. doi:10.1097/IAE.0b013e31828991b2.

Reticular Macular Disease is Associated with Multilobular Geographic Atrophy in Age-Related Macular Degeneration

Luna Xu, MD¹, Anna M. Blonska, MD¹, Nicole M. Pumariega, MS¹, Srilaxmi Bearely, MD, MHS¹, Mahsa A. Sohrab, MD¹, Gregory S. Hageman, PhD², and R. Theodore Smith, MD, PhD³

¹Department of Ophthalmology, E.S. Harkness Eye Institute, Columbia University, New York, NY

²Department of Ophthalmology and Visual Sciences, John A. Moran Eye Center, University of Utah, Salt Lake City, UT

³Department of Ophthalmology, New York University Langone Medical Center, New York, NY

Abstract

Purpose—To investigate the incidence of reticular macular disease (RMD), a subphenotype of age-related macular degeneration (AMD), in multilobular geographic atrophy (GA) and its relation to GA progression.

Methods—157 eyes of 99 subjects with AMD, primary GA, and good-quality autofluorescence (AF) and/or infrared (IR) images were classified into unilobular GA (1 lesion) or multilobular GA (≥ 2 distinct and/or coalescent lesions). 34 subjects (50 eyes) had serial imaging. We determined the spatiotemporal relationships of RMD to GA and GA progression rates in 5 macular fields.

Results—144/157 (91.7%) eyes had multilobular GA, 95.8% of which exhibited RMD. In subjects with serial imaging, the mean GA growth rate significantly differed between the unilobular and multilobular groups ($0.40 \text{ mm}^2/\text{yr}$ vs. $1.30 \text{ mm}^2/\text{yr}$, $p < 0.001$). Of the macular fields in these eyes, 77.1% of fields with RMD at baseline showed subsequent GA progression, while 53.4% of fields without RMD showed progression ($p < 0.001$). Percentage of fields with RMD significantly correlated with GA progression rate ($p = 0.01$).

Conclusion—AF and IR imaging demonstrates that RMD is nearly always present with multilobular GA in AMD. Further, GA lobules frequently develop in areas of RMD, suggesting progression of a single underlying disease process.

Keywords

age-related macular degeneration; geographic atrophy; reticular macular disease; scanning laser ophthalmoscopy; autofluorescence imaging; progression

Correspondence/reprints should be addressed to: R. Theodore Smith, MD, PhD, Department of Ophthalmology, New York University Langone Medical Center, 462 First Avenue – NBV 5N18, New York, NY 10016, roland.smith@nyumc.org, Phone: (646) 501-4246, Fax: (212) 263-8749.

Parts of the findings of this paper were presented at the Association for Research in Vision and Ophthalmology 2012 Conference in Fort Lauderdale, FL.

Financial disclosures: Dr. Hageman is on the Ophthalmology Clinical Advisory Board of Sequenom, Inc., and has financial interest in Ophtherion, Inc.

Conflict of interest: The authors have no conflicts of interest to disclose.

Introduction

Reticular pseudodrusen (RPD) have been associated with late-stage age-related macular degeneration (AMD) since their initial identification using blue light photography¹ and their inclusion in the Wisconsin Grading System using color fundus (CF) photographs to grade AMD.² The first comprehensive study of RPD found a higher incidence of choroidal neovascularization (CNV) within this subset of patients.³ Several subsequent studies found further associations between RPD and CNV,⁴⁻⁷ although a comprehensive epidemiological study of RPD found an overall increased incidence of late-stage AMD in patients with RPD without preference for CNV over atrophic AMD.⁸

With advances in imaging technology since RPD were first reported, characteristic reticular patterns were also noted in indocyanine green angiography (ICG)⁹ and autofluorescence (AF)¹⁰ images, leading to the broader definition of reticular macular disease (RMD). RMD, which includes RPD, is an entity with a characteristic presentation of reticular patterns in each of several imaging modalities, including AF, ICG, CF, red free (RF), and infrared (IR) imaging.¹¹ We will use the broader term “RMD” throughout to refer to the disease process in question, with the understanding that, in previous literature, the term “RPD” has been used specifically for the disease presentation in CF/RF photography.^{2-5, 8, 9} Recent studies have used spectral domain optical coherence tomography (SD-OCT) to characterize the lesions of RMD as subretinal deposits,¹²⁻¹⁶ but the matter is far from being settled. Zweifel et al. compared their SD-OCT findings to *previously* published histopathologic findings in 3 unrelated eyes showing subretinal deposits, but none of these eyes had a clinical diagnosis of RPD.¹² In contrast to this finding, the first histopathologic correlation in an eye with a clinical diagnosis of RPD by Arnold et al. demonstrated significant loss of the small vessels of the middle choroidal layer and increased spacing between the large choroidal veins, suggesting a choroidal etiology for RPD.³ Recently, Sarks et al.¹⁷ reported pathology from an eye clinically diagnosed with RPD and found material in the subretinal space, yet they also stated that subretinal deposits are not exclusively associated with RPD and therefore kept the term “reticular pseudodrusen.” Even more recently, Sohrab et al.¹⁸ did *not* find co-localization between IR reticular lesions and apparent subretinal deposits in SD-OCT, but they *did* find that these lesions co-localized to the intervascular choroidal stroma in en face SD-OCT C-sections. Thus whether subretinal deposits in SD-OCT correspond to RPD is controversial, and for this reason, we prefer to use the more general term “reticular macular disease” to refer to the disease process and the term “reticular pseudodrusen” to refer to its specific presentation in color, red free, and blue light photography, at least until these matters are settled more definitively.

With multimodal imaging, the reported prevalence of RMD and its association with late-stage AMD continue to increase.^{8-14, 16} For example, the prevalence of RMD in geographic atrophy (GA) in AF imaging has recently been reported to be as high as 62%.¹⁹ Herein we undertake a detailed study of the spatial and temporal relationship of RMD to GA with both AF and IR imaging.

Methods

Subjects and Image Acquisition

This study was approved by the Institutional Review Board of Columbia University and adhered to the tenets of the Declaration of Helsinki. All AF and IR images acquired at Columbia University E.S. Harkness Eye Institute on the Heidelberg HRA/HRA2 and Spectralis confocal scanning laser ophthalmoscope (SLO)-OCT (Heidelberg Engineering, Inc., Heidelberg, Germany) were retrospectively reviewed. These devices record AF images with an excitation wavelength of 488 nm and a barrier filter of 500 nm and IR reflectance

images with an excitation wavelength of 820 nm ($30^\circ \times 30^\circ$ field of view, image resolution 768×768 pixels). To ensure the best image quality (well-defined vasculature and GA margins), photographers at our institution acquired the highest possible number of frames (up to 30 frames) to obtain a mean image. The number of frames depended on the patient's fixation. Either the automatic real time mode or the mean image mode was used for all AF and IR image acquisition.

From this review, 288 subjects 60 years or older with focal hypoautofluorescent and/or hyperreflectant lesions were identified. Of these 288 subjects, 99 subjects (157 eyes) with primary GA and AMD were identified. GA was characterized by retinal pigment epithelium loss demonstrated by focal hypoautofluorescence and/or hyperreflectance at least $300 \mu\text{m}$ in diameter.^{20, 21} Comparison with CF or IR images was also important in order to avoid inaccurate identification of drusen or macular pigment as GA in AF images.²² Further, GA was required to be *primary* in that it was *not* related to any prior history of retinal surgery, laser treatment, other macular diseases of the studied eye, myopia greater than 6 diopters, or development of CNV prior to GA. Ascertainment of primary GA was based on review of the complete medical record, which was available in every case from the referring ophthalmologist at the Eye Institute, to document the absence of each exclusion criterion. In particular, eyes with lesions suspicious for prior CNV were always excluded. If a subject had at least 2 serial images available, with at least 6 months between the images, the subject was selected for longitudinal review. We found 34 such subjects (50 eyes).

Classification of Unilobular and Multilobular Primary GA

Eyes with primary GA were classified into 2 phenotypic patterns, unilobular and multilobular, based on the pattern of atrophy in all available images and the number of atrophic areas. Unilobular GA was defined as 1 contained area of atrophy within the $6000\text{-}\mu\text{m}$ macular region. Multilobular GA, on the other hand, was defined as 2 or more lobules of atrophy, distinct or merged. The AF gray levels in lobules of evident multilobular disease were not required to be identical. If there were serial images of a given eye, it was classified as multilobular if it had multilobular GA at any time point.

For our purposes, the term “lobule” refers to a well-circumscribed region whose borders are nearly circular or to joined areas with smooth, curved borders. We have chosen the term “multilobular,” rather than the more general term “multifocal,” because it is applicable to almost all the lesions we have studied and conveys a helpful image to the reader. It is also possible that this morphology reflects an underlying disease substrate, e.g., the choroidal vasculature, but the terminology here is meant only to be descriptive.

Definition of RMD

RMD is a disease entity with stereotypical presentations in multiple imaging modalities; RPD are one manifestation of RMD.¹¹ RPD were first described as yellow or light interlacing networks appearing in fundus photographs.¹ Later they were found to be better visualized with RF and SLO (AF and IR) imaging.^{3, 5} In CF and corresponding RF images, RPD appear as low-contrast, well-defined networks ranging from 125 to $250 \mu\text{m}$ in width.^{1, 3, 11} In AF and IR images, RMD appears as a regular pattern of low-contrast hypoautofluorescent or hyporeflectant lesions in a circumscribed area, against a background of mildly elevated autofluorescence or reflectance.^{10, 11}

Many eyes with RMD also have ordinary soft drusen, and the fact that they may occur together in the same eye with AMD means that it is important to distinguish them. Fortunately, there are usually distinguishing features that make this possible. For example, we used Adobe Photoshop CS3 (Adobe Systems, Inc., San Jose, CA) to examine available

CF images with contrast enhancement and to examine them in the blue channel to distinguish soft drusen from RPD. RPD in CF images are often better visualized with contrast enhancement,¹¹ and they are more visible in the blue channel than soft drusen.^{3, 5, 11, 12, 14, 15} Soft drusen in IR images tend to be hyperreflectant, whereas the lesions of RMD are always hyporefectant. Soft drusen tend to be scattered, with variable shapes and sizes.

The lesions of RMD in IR and AF images occur in well-defined territories, usually superior and temporal, in uniformly spaced patterns and uniform sizes.⁸ It has been shown that a reticular pattern can also occur nasally to the optic disc.¹⁹ IR imaging can better demonstrate a reticular pattern in the central macula compared to other modalities.¹¹ We screened the subjects in our study for RMD using all available AF and IR images, and we defined RMD as a characteristic pattern encompassing at least 2 contiguous disc areas in at least 1 imaging modality, an internally validated, previously described methodology.¹¹ In addition to SLO imaging, other investigators require SD-OCT imaging to diagnose RMD, in particular, a pattern of disruption of the inner segment/outer segment junction.¹²⁻¹⁶ We have not consistently seen this pattern in SD-OCT slices through areas clearly involved by RMD in both AF and IR imaging¹⁸ and therefore do not require it for diagnosis. Examples of unilobular and multilobular GA with RMD in both AF and IR imaging are presented in Figures 1 and 2, respectively. Evaluation for RMD was done independently by 2 graders (LX and NMP), and any discrepancies were resolved by a senior grader (RTS) as described previously.¹¹

Analysis of GA Progression in Serial AF and IR Images

The AF and IR images were cropped to the central 6000- μm region, and serial images were registered using a graphical user interface and custom software based on Harris corner point detection.²³ Automated measurements of the GA area in both modalities were performed using another customized retinal image analysis tool^{24, 25} in which a user manually selected a small area of GA and a normal retinal area and Bayesian inference then segmented the remaining area of GA. Manual revision was performed when needed. The GA area was calculated as a percentage of the total image and in mm^2 . If a subject had more than 2 serial images acquired during the duration of the study, with at least 6 months between the images, the GA progression rate was calculated as the slope of the best-fitted line. The GA progression rate was also calculated on the square root scale, using the square root transformation method, as described by Yehoshua et al.²⁶ This was done to compensate for the effect that different initial GA sizes may have had on progression.

We modified the grid from the Wisconsin Grading System²⁷ and used it to divide the images for analysis into superior, temporal, inferior, and nasal quadrants and a central 3000- μm -diameter circle (Figure 3). The quadrants and the middle zone were collectively referred to as "macular fields." Each of these 5 macular fields was graded for the presence of RMD in the initial image and for the progression or new development of GA in the subsequent image(s). AF images were preferentially used for this analysis, but IR images were used when AF images were of lesser quality (for example, due to cataract). In cases in which a given field had no recognizable reticular lesions on AF or IR, RMD was graded as absent. If a given field had GA covering more than 80% of the field, the RMD status was deemed ungradable. The fields with and without RMD were tabulated, and the number of fields of each type in which GA was progressive was determined (Figure 3).

In analyzing whether GA progressed in a particular field, straightforward, simply defined criteria were applied. If the borders of the GA lesions were essentially unchanged in the segmented, registered images in a given field, then GA progression was graded minimal to none; otherwise, GA was graded as progressive. An enlargement of an existing lesion that

crossed over to an adjacent field was counted as progression in the new field. If a new lobe grew in a previously noninvolved field, this was also counted as progression in the new field. Evaluation for GA progression was done independently by 2 graders (LX and NMP), and any discrepancies were resolved by a senior grader (RTS).

Statistical Analysis

The χ^2 test for categorical variables in univariate analysis was used to determine the association of RMD with primary GA. SPSS (SPSS, Inc., Chicago, IL) was used to perform the Mann-Whitney nonparametric test to compare the statistical distribution of parameters such as age. The student t-test was used to compare the GA progression rates between unilobular and multilobular groups. The χ^2 test was used to compare, for all fields taken together, the percent of fields with RMD that showed GA progression to the percent of fields without RMD that showed GA progression. Our χ^2 tests and t-tests were performed using Excel (Microsoft Corp., Redmond, WA).

A multivariate linear regression model for the numerical rate of total GA area growth was also developed using SPSS. The model incorporated the percent of retinal fields with RMD (x_1) and baseline GA size (x_2) as independent predictors of GA growth rate (y) such that $y = 0 + 1*x_1 + 2*x_2$. This model was applied to all eyes in the study ($n=50$) and then to 1 eye per subject ($n=34$).

In a separate analysis, study eyes were grouped by follow-up intervals in 6-month increments (e.g., eyes which were followed up at 6 months after the initial visit, 7-12 months, 13-18 months, etc.), and growth rates on the square root scale with their standard deviations were calculated. The test-retest variability in GA growth measurement was estimated by regressing the growth rates on the square root scale against their standard deviations, using methods previously described by Yehoshua et al.²⁶ The regression line with a mean growth of zero represented the test-retest variability.

Results

All SLO Images

The mean age of the subjects was 81.8 \pm 7.2 years, and 77/99 (77.8%) were female. 144/157 (91.7%) eyes showed multilobular GA, and 13/157 (8.3%) showed unilobular GA. Of the eyes with multilobular GA, 138/144 (95.8%) exhibited RMD. Of all eyes, 146/157 (93.0%) exhibited RMD in SLO imaging, with most (130/155 or 83.9%, 2 eyes ungradable) exhibiting reticular IR and/or AF patterns in the superior arcade (Figures 1, 2, 4). The interobserver agreement for reticular lesions was 95.4% with a kappa of 0.88.

131/157 eyes (83.4%) had both AF and IR images available, while only 13/157 (8.3%) and 13/157 (8.3%) had either AF or IR, respectively. For the eyes with CF photography available at baseline, only 77/123 (62.6%) exhibited RMD in CF images, while 114/123 (92.7%) exhibited RMD in AF or IR images. We observed RMD surrounding the optic disc in many of the images that showed the peripapillary retina. Five eyes with unilobular GA had no signs of RMD. The combined spatial distribution of reticular lesions in both SLO imaging modalities (i.e., lesions visible in *either* AF *or* IR) is shown in Figure 5.

The subjects with multilobular GA showed a slightly higher mean age at baseline (82.5 \pm 6.9 years) than the subjects with unilobular GA (77.0 \pm 8.1 years, $p = 0.05$). Despite the preponderance of women with GA in the entire group, only 6/11 (54.5%) subjects with unilobular GA were female, compared to 71/88 (80.7%) subjects with multilobular GA ($p = 0.049$). There was no significant difference between subjects with multilobular GA and

subjects with unilobular GA regarding the specific location of GA at baseline (foveal vs. extrafoveal). See Table 1.

Serial SLO Images

AF and/or IR serial images were available for 34 subjects (50 eyes). The mean duration of follow-up was 27.2 months (range 6 - 51 months). At baseline, 5/50 (10.0%) eyes had unilobular GA and 45/50 (90.0%) eyes had multilobular GA. Of the total, 44/50 (88.0%) had RMD in at least 1 image. The mean GA size at baseline was 3.48 mm², with an interquartile range (IQR) of 0.55- 5.35 mm². The mean GA growth rate was 1.21 mm²/yr overall (SD 0.22, 95% confidence interval (CI) 0.99 – 1.43 mm²/yr). It was significantly different between the unilobular (0.40 mm²/yr, SD = 0.26, 95% CI 0.17-0.63 mm²/yr) and multilobular groups (1.30 mm²/yr, SD = 0.23, 95% CI 1.07 – 1.52mm²/yr) with significant $p < 0.001$. Age and gender did not influence GA progression. Peripapillary atrophic changes (including those that were not frank GA) were present in 45/50 (90.0%) eyes. 39/50 (78.0%) had extrafoveal GA at baseline; 6/39 (15.4%) of these eyes (all belonging to the multilobular group) progressed from extrafoveal to foveal GA.

Using square root transformation,²⁶ the overall growth rate was 0.34 mm/yr (SD = 0.08, 95% CI = 0.28- 0.41 mm/yr). The growth rate was 0.19 mm/yr (SD = 0.07, 95% CI = 0.13- 0.26 mm/yr) for the unilobular eyes and 0.36 mm/yr (SD = 0.07, 95% CI = 0.29- 0.43 mm/yr) for the multilobular eyes, with a statistically significant difference between the two groups by 2-tailed t-test ($p = 0.003$).

When study eyes were grouped by follow-up intervals in 6-month increments, the square root transformations of GA measurements for these subgroups showed that larger lesion sizes corresponded to greater variability in growth measurements. The test-retest variability in GA growth measurement was 0.03, and the slope of the regression line was 0.58; these were comparable to the test-retest variability and regression slope as published in the report of Yehoshua et al.²⁶

Qualitative observation revealed that the areas of atrophy were at various stages on the first and following visit(s). There was significant variability in disease severity, area of macular involvement, and rate of progression, but in every case GA lesions were formed from new and enlarging individual lobules. The most commonly observed pattern showed progressive growth and coalescence of the original smaller lobules into larger, continuous GA lesions, with new lesions appearing more peripherally (Figures 6, 7). Importantly, lesions that appeared in IR images to be single, large central lesions were instead often observed in AF images to be condensations of densely packed smaller lobules (Figure 6). There was a subgroup of subjects in which GA lesions remained relatively small and distinct, with separate lobules of atrophy enlarging and new atrophic foci forming.

In subsequent images, new atrophic lobules were less hypoautofluorescent than adjacent atrophic lobules in the initial AF image (Figure 6). Based on this finding, it appeared that different gray levels of atrophic lobules in a single non-serial image could also signify different stages of disease (Figure 2).

For quantitative analysis, each image was graded for the presence of RMD and GA progression in the 5 macular fields (250 fields total). 3/250 fields were deemed ungradable. Of the 247/250 gradable fields, 111/144(77.1%) fields with RMD at baseline showed subsequent GA progression, while 55/103 (53.4%) fields without RMD showed progression, a statistically significant difference ($p < 0.001$). See Table 2.

The multivariate linear regression model for GA area growth rate as a function of percent of retinal fields with RMD and baseline GA size yielded a regression coefficient of 0.42. The model accounted for 17.3% of the total variance in GA growth rate ($p = 0.01$). Controlling for baseline GA size in all study eyes, the percent of retinal fields with RMD approached significance in predicting the growth rate of GA ($p=0.06$). In the subanalysis that included only 1 eye per subject ($n=34$), the regression coefficient remained high at 0.374, and the model accounted for 14.0% of the total variance in GA progression ($p=0.10$).

Discussion

We report observations from SLO (AF and IR) images in a group of subjects with GA secondary to AMD. Careful examination of SLO images demonstrates that the majority of such GA is multilobular and that RMD is consistently present with the multilobular form. To our knowledge, this is the first report of a nearly universal presence of RMD in eyes with AMD and multilobular GA.

With improved imaging technologies, the reported rate of reticular disease in the literature has climbed steadily, from 21% in the Beaver Dam Study with CF photography⁸ to 62% most recently reported in the Geographic Atrophy Progression Study using SLO.¹⁹ However, the incidence in our cohort was much higher still, with 93.0% of all eyes with GA exhibiting RMD. One possible explanation is that our grading of RMD was more inclusive than other studies. We graded eyes as having RMD if 2 disc-diameters (DD) of characteristic lesions could be identified anywhere in the image, e.g., superior to the disc, not just between the arcades. Of note, in CF images, RMD could be identified in only 62.6% of all eyes with GA in our study, even with contrast enhancement in Adobe Photoshop, confirming that the combination of AF and IR imaging is more sensitive in detecting RMD in these subjects. Although RMD may be seen in AF imaging but not in IR imaging, or vice versa in a minority of cases, the marked spatial concordance of lesions in both modalities¹¹ is strong evidence that both modalities are detecting a single disease process.

Clarity is also required on another diagnostic matter. We rely on a validated, previously published method of grading SLO images (see Methods),^{6,11} but other investigators use additional SD-OCT criteria to define what they call “subretinal drusenoid deposits,”¹² an entity which may largely overlap with RMD. Our ongoing prospective study employs SD-OCT, and upcoming research may clarify the relationship between RMD and subretinal drusenoid deposits. Regardless of the underlying pathology, different diagnostic criteria will affect the conclusions, and all investigators need to define their criteria clearly.

We propose a unifying hypothesis to explain our observations: RMD and GA are not simply associated, but in fact RMD develops into multilobular GA with time as progression of a single underlying disease. This hypothesis is supported by the lesion architecture seen on SLO images in several ways. First, GA in AMD, when examined with AF imaging, is usually multilobular, composed of multiple smaller lobules coalescing together. Second, not only is multilobular GA highly associated with RMD, but also the individual lobules appear to enlarge over time in areas of reticular lesions. Indeed, we demonstrated a significant spatial correlation of progressive GA to macular fields with pre-existing RMD for 50 study eyes (Figure 3, Table 2), and total GA growth rate was significantly predicted by a model that included initial GA size and percent of macular fields with RMD. Third, the concept of progression from RMD to established GA is supported by the qualitative observation of progressively decreasing gray levels of these lesions in AF imaging: in individual images and in serial data, the low-contrast RMD lesions are the least hypoautofluorescent, early GA lesions are darker than RMD, and established GA lesions are darkest of all, consistent with progressive stages of disease (Figure 2). Hence, there are several ways in which imaging

suggests progression of a single process, from smaller to larger lesions (multiscale) and, at the same time, from earlier to more advanced lesions (multistage). This hypothesis also satisfies Occam's razor as the simplest explanation for all observed phenomena, although the underlying mechanism is as yet unknown.

Regarding the lobularity of GA, this study presents a greater incidence of multilobular than unilobular GA. Earlier papers based on CF photography reported the multilobular form as the minority classification.^{28,29} The present study clearly demonstrates a much better visualization of multilobular disease with SLO images, particularly AF images, than with CF images³⁰ (Figure 8). Indeed, the 11 subjects herein who had strictly unilobular GA had a significantly lower age at baseline than those with multilobular GA, and they were evenly divided between males and females, in contrast to the significant predominance of females in the multilobular group (Table 1), suggesting that purely unilobular GA may be a distinct phenotype.

This paper adds to the growing recognition of the importance of RMD in advanced AMD. Several papers have confirmed the strong association of RMD with CNV, but there is less in the literature about the dry form of AMD. The evidence herein supports the hypothesis that RMD may represent precursor lesions for both forms of advanced AMD. This paradigm could guide future work toward understanding these two apparently dichotomous pathways.

Limitations of the present study include its retrospective design and the fact that there was serial imaging on only 34 subjects from which to build a unifying hypothesis regarding RMD and multilobular GA by direct observation of lesion progression. Further, although observation of GA progression was based on AF images whenever possible, IR images were used if AF images were unavailable or of poor quality. Although there was a very strong link between GA progression and reticular disease in both image types, it would have been ideal to have had both AF and IR images for each subject.

The follow-up intervals in our study group covered a large range (6-51 months), which potentially could have biased our results if the GA progression rate varied with the follow-up interval. However, subgroup analysis of ranges of follow-up intervals did not suggest any trend.

The retrospective design might suggest a selection bias toward larger GA lesions, for example, if subjects with more advanced disease were more likely to get imaging. However, the mean GA progression rate of 1.21 mm²/yr observed herein was slightly lower than the mean rate reported in other studies^{26, 28, 31-33} and was also associated with a smaller mean initial lesion size (3.48 mm²) and a smaller IQR (0.55 - 5.35 mm²),^{26, 31, 33} suggesting that our study group did not have more advanced GA. Repeat analysis using square root transformation²⁶ showed that initial lesion size did not affect GA progression rate. The mean age of patients in this study was slightly older than, yet comparable to, published reports.^{26, 28, 31-34} There was a higher percentage of women in our study than in these other GA studies, but this may simply have been related to the older age of our group.

The strength of this study lies in the uniformity of the findings, with a nearly 100% association of RMD with multilobular GA. This is a far stronger association than previously reported and relies on careful examination of the posterior pole in images of multiple modalities at multiple time points. This also suggests a greater predictive value of RMD for advanced AMD than previously believed, because the overall incidence of RMD in early AMD is only around 8% as found previously by our group using the same definition of RMD applied herein.⁶

In summary, we have presented evidence that multilobular GA in AMD is almost always associated with reticular macular disease. Study of serial SLO images further suggests that this is not simply an association but that lobules of GA develop in areas of RMD and may represent progression of a single underlying disease process. Prospective studies of larger cohorts of patients with GA, particularly histopathologic study of well-documented cases of reticular disease, are clearly indicated to assess these possibilities. In general, SLO imaging demonstrates that the high-risk phenotype of RMD is much more ubiquitous than previously realized and deserves further careful study.

Acknowledgments

Supported by grants from The New York Community Trust (New York, NY) (RTS); National Eye Institute (Bethesda, MD) grants R01 EY015520 (RTS) and R24 EY017404 (GSH); unrestricted grants to the E.S. Harkness Eye Institute and the University of Utah Department of Ophthalmology and Visual Sciences from Research to Prevent Blindness (New York, NY); the Kaplen Foundation (SB); and the Doris Duke Clinical Research Fellowship Program (LX). The funding organizations had no role in the design or conduct of this research.

References

- Mimoun G, Soubrane G, Coscas G. Macular drusen. *J Fr Ophthalmol*. 1990; 13:511–30.
- Klein R, Davis MD, Magli YL, et al. The Wisconsin Age-Related Maculopathy Grading System. *Ophthalmology*. 1991; 98:1128–34. [PubMed: 1843453]
- Arnold JJ, Sarks SH, Killingsworth MC, Sarks JP. Reticular pseudodrusen: a risk factor in age-related maculopathy. *Retina*. 1995; 15:183–91. [PubMed: 7569344]
- Prenner JL, Rosenblatt BJ, Tolentino MJ, et al. Risk factors for choroidal neovascularization and vision loss in the fellow eye study of CNVPT. *Retina*. 2003; 23:307–14. [PubMed: 12824829]
- Cohen SY, Dubois L, Tadayoni R, et al. Prevalence of reticular pseudodrusen in age-related macular degeneration with newly diagnosed choroidal neovascularization. *Br J Ophthalmol*. 2007; 91:354–9. [PubMed: 16973663]
- Smith RT, Chan JK, Busuioic M, et al. Autofluorescence characteristics of early, atrophic, and high-risk fellow eyes in age-related macular degeneration. *Invest Ophthalmol Vis Sci*. 2006; 47:5495–504. [PubMed: 17122141]
- Hwang JC, Chan JW, Chang S, Smith RT. Predictive value of fundus autofluorescence for development of geographic atrophy in age-related macular degeneration. *Invest Ophthalmol Vis Sci*. 2006; 47:2655–61. [PubMed: 16723483]
- Klein R, Meuer SM, Knudtson MD, et al. The epidemiology of retinal reticular drusen. *Am J Ophthalmol*. 2008; 145:317–26. [PubMed: 18045568]
- Arnold JJ, Quaranta M, Soubrane G, et al. Indocyanine green angiography of drusen. *Am J Ophthalmol*. 1997; 124:344–56. [PubMed: 9439360]
- Lois N, Owens SL, Coco R, et al. Fundus autofluorescence in patients with age-related macular degeneration and high risk of visual loss. *Am J Ophthalmol*. 2002; 133:341–9. [PubMed: 11860971]
- Smith RT, Sohrab MA, Busuioic M, Barile G. Reticular macular disease. *Am J Ophthalmol*. 2009; 148:733–43. [PubMed: 19878758]
- Zweifel SA, Spaide RF, Curcio CA, et al. Reticular pseudodrusen are subretinal drusenoid deposits. *Ophthalmology*. 2010; 117:303–12. [PubMed: 19815280]
- Schmitz-Valckenberg S, Steinberg JS, Fleckenstein M, et al. Combined confocal scanning laser ophthalmoscopy and spectral-domain optical coherence tomography imaging of reticular drusen associated with age-related macular degeneration. *Ophthalmology*. 2010; 117:1169–76. [PubMed: 20163861]
- Zweifel SA, Imamura Y, Spaide TC, et al. Prevalence and significance of subretinal drusenoid deposits (reticular pseudodrusen) in age-related macular degeneration. *Ophthalmology*. 2010; 117:1775–81. [PubMed: 20472293]

15. Spaide RF, Curcio CA. Drusen characterization with multimodal imaging. *Retina*. 2010; 30:1441–54. [PubMed: 20924263]
16. Querques G, Querques L, Martinelli D, et al. Pathologic insights from integrated imaging of reticular pseudodrusen in age-related macular degeneration. *Retina*. 2011; 31:518–26. [PubMed: 21150696]
17. Sarks J, Arnold J, Ho IV, et al. Evolution of reticular pseudodrusen. *Br J Ophthalmol*. 2011; 95:979–85. [PubMed: 21109695]
18. Sohrab MA, Smith RT, Salehi-Had H, et al. Image registration and multimodal imaging of reticular pseudodrusen. *Invest Ophthalmol Vis Sci*. 2011; 52:5743–8. [PubMed: 21693600]
19. Schmitz-Valckenberg S, Alten F, Steinberg JS, et al. Reticular drusen associated with geographic atrophy in age-related macular degeneration. *Invest Ophthalmol Vis Sci*. 2011; 52:5009–15. [PubMed: 21498612]
20. Fleckenstein M, Charbel Issa P, Helb HM, et al. High-resolution spectral domain-OCT imaging in geographic atrophy associated with age-related macular degeneration. *Invest Ophthalmol Vis Sci*. 2008; 49:4137–44. [PubMed: 18487363]
21. Sarks JP, Sarks SH, Killingsworth MC. Evolution of geographic atrophy of the retinal pigment epithelium. *Eye (Lond)*. 1988; 2(Pt 5):552–77. [PubMed: 2476333]
22. Sunness JS, Ziegler MD, Applegate CA. Issues in quantifying atrophic macular disease using retinal autofluorescence. *Retina*. 2006; 26:666–72. [PubMed: 16829810]
23. Chen J, Smith R, Tian J, Laine AF. A novel registration method for retinal images based on local features. *Conf Proc IEEE Eng Med Biol Soc*. 2008; 2008:2242–5. [PubMed: 19163145]
24. Lee N, Laine AF, Smith RT. Bayesian transductive Markov random fields for interactive segmentation in retinal disorders. *IFMBE Proc*. 2009; 25:227–30.
25. Lee N, Smith RT, Laine AF. Interactive segmentation for geographic atrophy in retinal fundus images. *Conf Rec Asilomar Conf Signals Syst Comput*. 2008; 2008(42):655–8. [PubMed: 21866210]
26. Yehoshua Z, Rosenfeld PJ, Gregori G, et al. Progression of geographic atrophy in age-related macular degeneration imaged with spectral domain optical coherence tomography. *Ophthalmology*. 2011; 118:679–86. [PubMed: 21035861]
27. Bird AC, Bressler NM, Bressler SB, et al. The International ARM Epidemiological Study Group. An international classification and grading system for age-related maculopathy and age-related macular degeneration. *Surv Ophthalmol*. 1995; 39:367–74. [PubMed: 7604360]
28. Klein R, Meuer SM, Knudtson MD, Klein BE. The epidemiology of progression of pure geographic atrophy: The Beaver Dam Eye Study. *Am J Ophthalmol*. 2008; 146:692–9. [PubMed: 18672224]
29. Sunness JS, Margalit E, Srikumaran D, et al. The long-term natural history of geographic atrophy from age-related macular degeneration: enlargement of atrophy and implications for interventional clinical trials. *Ophthalmology*. 2007; 114:271–7. [PubMed: 17270676]
30. Dhanif AA, Lederer ED, Ghodasra JH, et al. Comparison of color fundus photographs and fundus autofluorescence images in measuring geographic atrophy area. *Retina*. 2012; 32:1884–91. [PubMed: 22547167]
31. Holz FG, Bindewald-Wittich A, Fleckenstein M, et al. Progression of geographic atrophy and impact of fundus autofluorescence patterns in age-related macular degeneration. *Am J Ophthalmol*. 2007; 143:463–72. [PubMed: 17239336]
32. Bearely S, Khanif AA, Lederer DE, et al. Use of fundus autofluorescence images to predict geographic atrophy progression. *Retina*. 2011; 31:81–6. [PubMed: 20890245]
33. Lindblad AS, Lloyd PC, Clemons TE, et al. Change in area of geographic atrophy in the Age-Related Eye Disease Study: AREDS report number 26. *Arch Ophthalmol*. 2009; 127:1168–74. [PubMed: 19752426]
34. Sunness JS, Bressler NM, Tian Y, et al. Measuring geographic atrophy in advanced age-related macular degeneration. *Invest Ophthalmol Vis Sci*. 1999; 40:1761–9. [PubMed: 10393046]

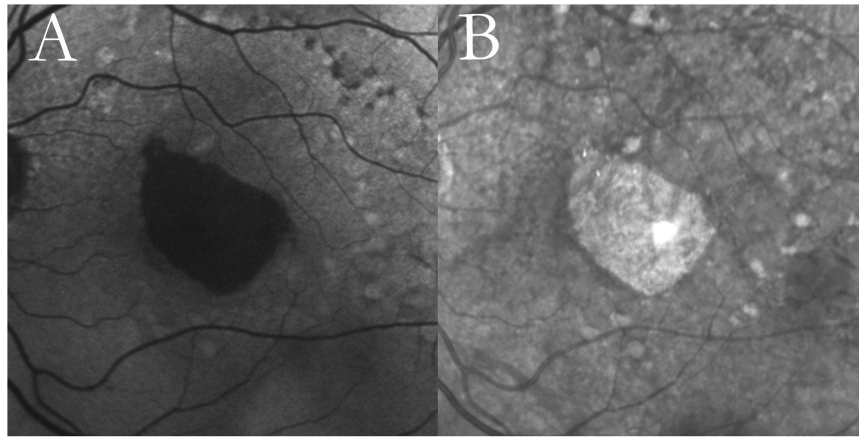


Figure 1. Unilobular geographic atrophy (GA) with reticular macular disease (RMD) Autofluorescence (**A**) and infrared (**B**) images from a 68-year-old female with age-related macular degeneration showing unilobular GA. Both modalities show RMD around the atrophic lesion and temporally to the optic disc, as well as large soft drusen more peripherally.

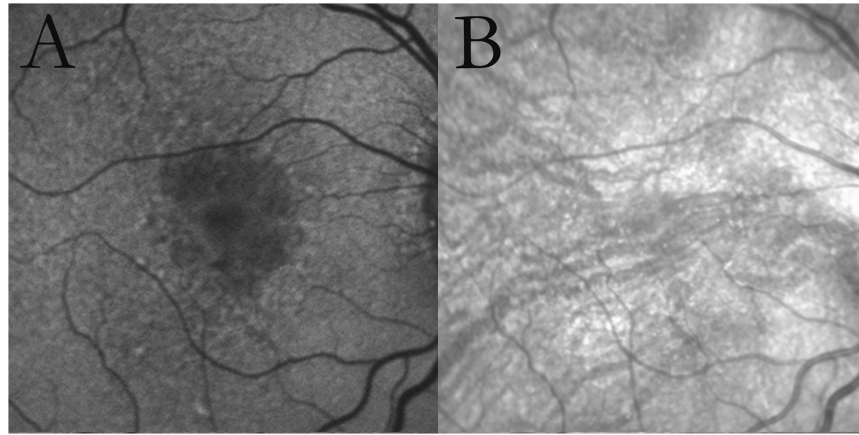


Figure 2. Multilobular geographic atrophy (GA) with reticular macular disease (RMD)
Autofluorescence (**A**) and infrared (**B**) images from an 80-year-old female with age-related macular degeneration showing multilobular GA. In autofluorescence imaging, the lobules demonstrate different gray levels, possibly representing different stages of atrophy. RMD is seen surrounding the atrophy in both modalities.

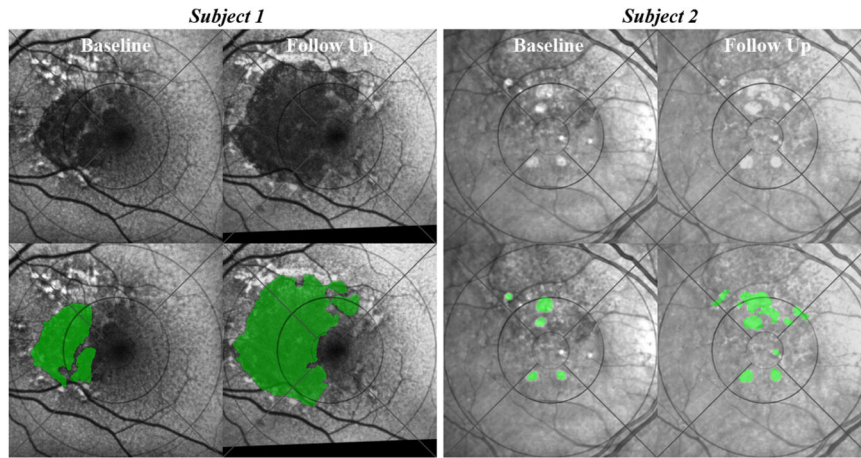


Figure 3. Grading by macular field of geographic atrophy (GA) progression relative to reticular macular disease (RMD)

The grids show the macula divided by circles into 6000-, 3000-, and 1000- μm -diameter zones and by lines into superior, temporal, inferior, and nasal quadrants further delimited by the middle and outer circles. Grading was done in 5 fields: in each quadrant and within the middle 3000- μm -diameter circle. The 1000- μm -diameter circle was not used for the analyses in this study. **(Subject 1, top row)** Baseline (**left**) and 2-year follow-up (**right**) autofluorescence images of the left eye from an 84-year-old female. **(Subject 1, bottom row)** The corresponding segmented and graded images initially showed GA present in all fields except the temporal quadrant and RMD present in all fields (**left**). Two years later (**right**), GA progressed in the superior, inferior, nasal, and central fields but not temporally despite RMD. Hence, in Subject 1, 4 of 5 fields with RMD showed GA progression. **(Subject 2, top row)** Baseline (**left**) and 2-year follow-up (**right**) infrared images of the right eye from an 83-year-old female. **(Subject 2, bottom row)** The corresponding segmented and graded images initially showed GA present superiorly and centrally and RMD definitely present in the superior and central fields (**left**). The nasal field had no recognizable reticular lesions, and RMD was graded as absent. Two years later (**right**), GA definitely progressed in the superior and central fields, with minimal to no growth in the nasal, inferior, and temporal fields. Hence, in Subject 2, 2 of 2 fields with RMD showed GA progression, and 3 of 3 fields without RMD did not.

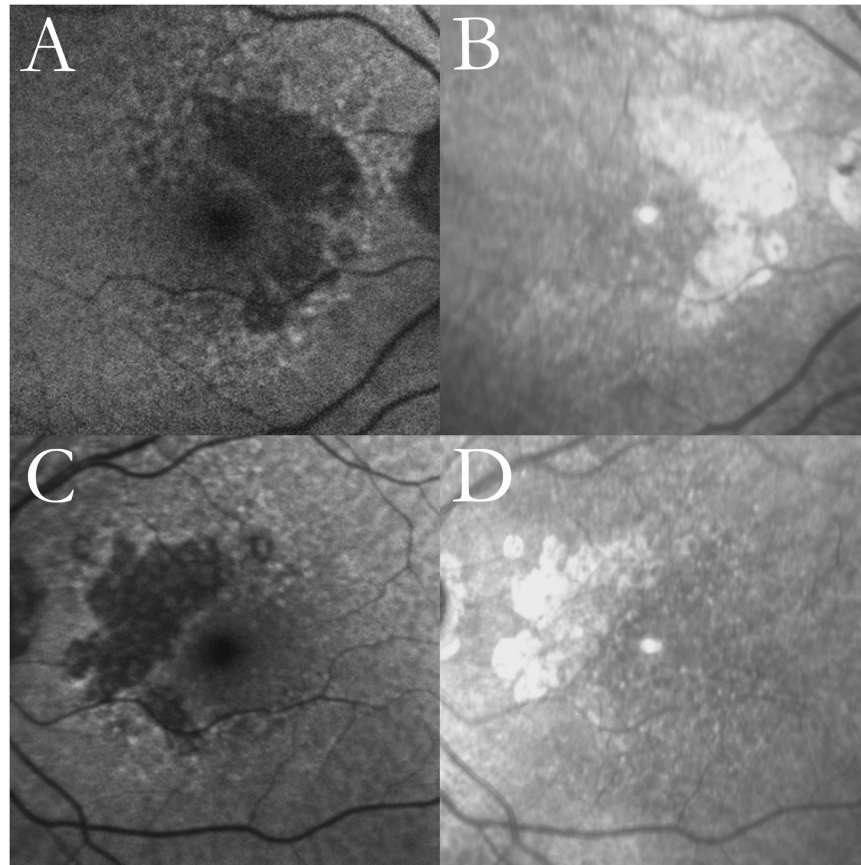


Figure 4. Bilateral multilobular geographic atrophy (GA) with reticular macular disease (RMD) Autofluorescence images of the right eye (**top left**) and the left eye (**bottom left**) of a 90-year-old female show dark, well-defined lobules of atrophy with surrounding RMD; large soft drusen are visible, especially above the edges of GA. Infrared images of the right eye (**top right**) and the left eye (**bottom right**) show prominent RMD, temporally to the optic disc and around the hyperreflective atrophic lesions, and large soft drusen.

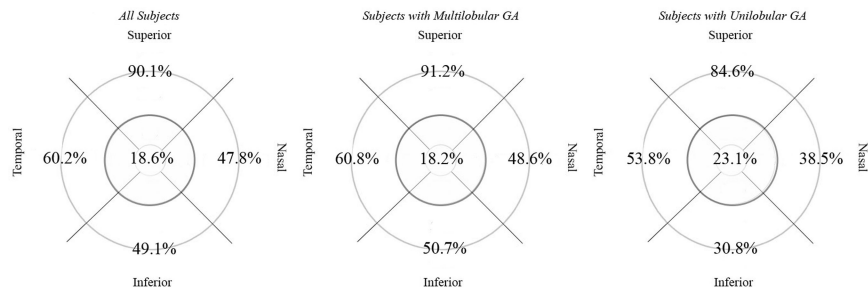


Figure 5. Combined distribution of reticular lesions in scanning laser ophthalmoscopy (autofluorescence and infrared) images for study subjects with reticular macular disease (RMD) and primary geographic atrophy (GA)

Distribution of RMD, when present, in all subjects, subjects with multilobular GA, and subjects with unilobular GA. For subjects with serial scans, only the initial set of scans with RMD was included in this analysis. RMD was most frequently noted outside the 3000- μ m-diameter circle (middle circle in darker grey) near the superior arcades.

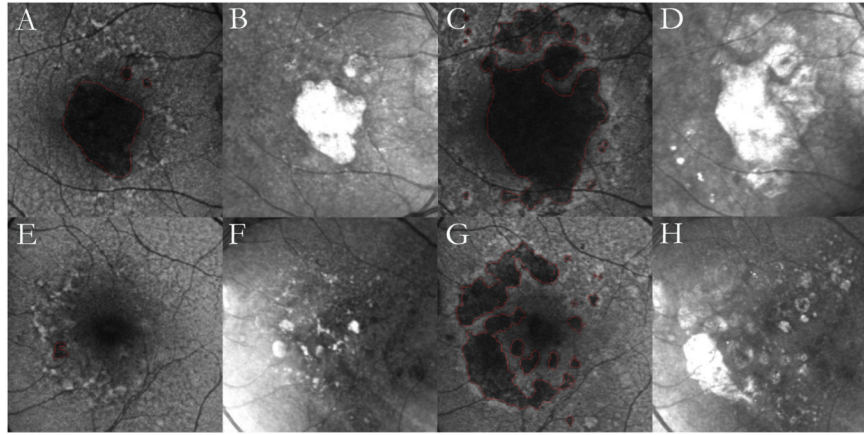


Figure 6. Progression of multilobular geographic atrophy (GA) over a period of 3 years (**Top row**) Right eye. (**Bottom row**) Left eye. (**Columns 1, 2**) Initial autofluorescence (AF) and infrared (IR) images. The individual GA lobules in the AF images are outlined in red using our user-interactive GA segmentation tool.^{24, 25} (**Columns 3, 4**) Follow-up AF and IR images after 3 years. The large central atrophic lesion in the right eye is present both initially and finally as seen in AF (**top row, columns 1, 3**) and IR (**top row, columns 2, 4**) scans; the GA in this eye appears to be a coalescence of densely packed atrophic lobules. The initial AF scan of the left eye (**bottom left**) shows prominent reticular macular disease in all quadrants with a small lesion of GA beginning to form within it. The atrophic areas are less apparent in the IR images (**bottom row, columns 2, 4**) compared to the well-outlined lobules of atrophy observed in the AF images (**bottom row, columns 1, 3**). After 3 years, there are significant new lobules of GA evident in all quadrants of the left eye.

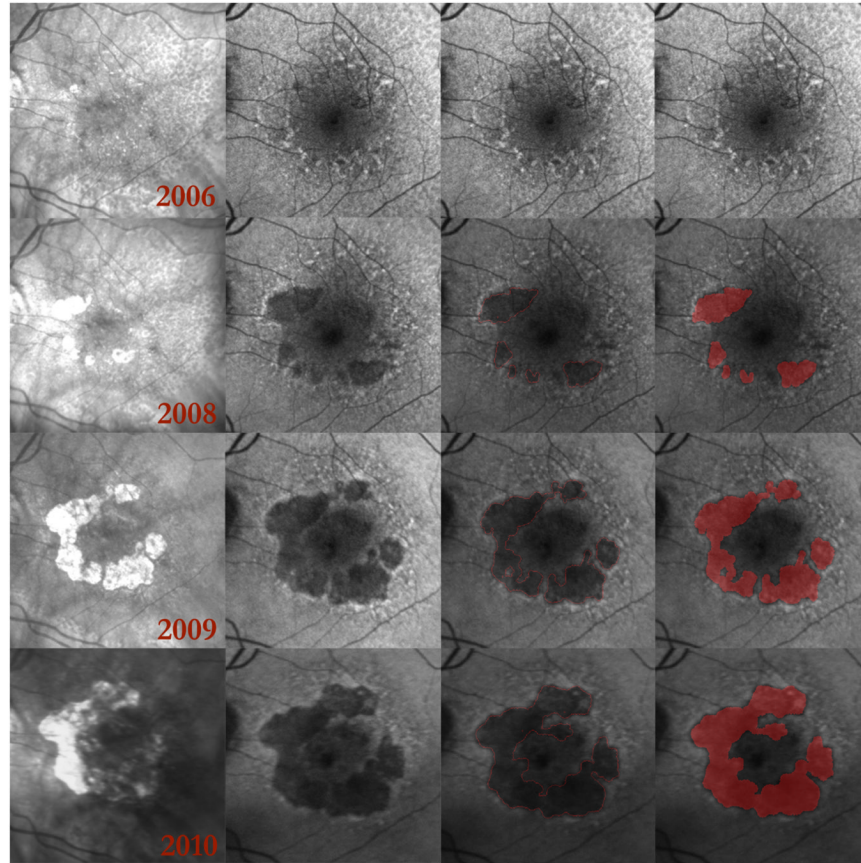


Figure 7. Multilobular geographic atrophy (GA) and reticular macular disease (RMD) over 4 years presented as a multiscale, multistage disease continuum

Each row represents 1 year of serial infrared (IR) and autofluorescence (AF) images. **(Column 1)** Serial IR images show enlargement of GA. **(Column 2)** Serial AF images show RMD (small-scale, early lesions) becoming gradually more hypoautofluorescent and coalescing into lobes of early GA (larger scale, later-stage lesions), which further coalesce and become even more hypoautofluorescent as they progress to mature GA (large-scale, end-stage lesions). Note that the AF lesions have distinct, decreasing gray scales as they progress from RMD to lobules of early GA and on to fully developed GA. The IR images do not show this distinction. The end-stage AF lesions (2010) are closely surrounded by irregular margins of elevated AF that in turn are surrounded by RMD. At each stage, RMD is clearly visible at the margins of the GA. **(Column 3)** The GA lesions in the serial AF images from Column 2 were outlined in red.^{24, 25} The segmentation included both early- and end-stage GA and included all areas of defined atrophy in the IR scans. **(Column 4)** Red masks were created in MATLAB R2007 (Mathworks, Natick, MA) for the serial AF images in Column 2 to measure the growth of atrophic lesions over 4 years.

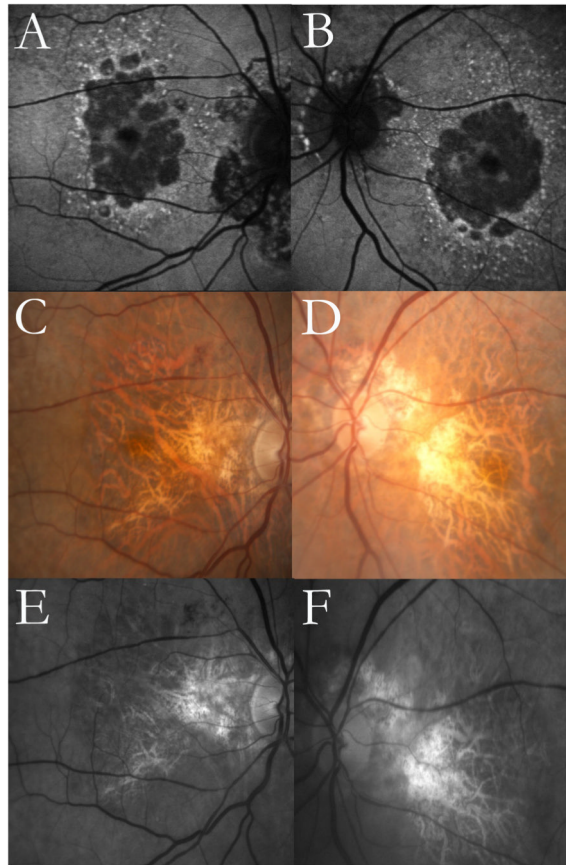


Figure 8. Multilobular geographic atrophy (GA) demonstrated in autofluorescence (AF) imaging but not in color fundus (CF) or red free (RF) photography

Images from an 88-year-old female with age-related macular degeneration. Multilobular GA and reticular macular disease (RMD) around the atrophic lobules are clearly visible in the AF images (**top row**). The CF (**middle row**) and RF (**bottom row**) images do not show the multilobular nature of the GA but do show RMD superotemporally in both eyes. Peripapillary atrophy is present in both eyes in all image modalities.

Table 1

Statistical analysis comparing subjects with multilobular geographic atrophy (GA) and subjects with unilobular GA.

Characteristics	All Subjects	Multilobular	Unilobular	P Value
Sample Size (%)	99	88/99 (88.9)	11/99 (11.1)	
Eyes (%)	157	144/157 (91.7)	13/157 (8.3)	
Age, Yrs, Mean (SD)	81.8 (7.2)	82.5 (6.9)	77.0 (8.1)	0.05
Women (%)	77/99 (77.8)	71/88 (80.7)	6/11 (54.5)	0.049
Eyes with Foveal GA (%)	74/157 (47.1)	66/144 (45.8)	8/13 (61.5)	0.278
Eyes with RMD in SLO Images (%)	146/157 (93.0)	138/144 (95.8)	8/13 (61.5)	3.49E-06
Eyes with RMD in CF Photography (%)	77/123 (62.6)	72/111 (64.9)	5/12 (41.7)	0.115

Yrs, years; SD, standard deviation; RMD, reticular macular disease; SLO, scanning laser ophthalmoscope; CF, color fundus.

Table 2

Overall pattern of geographic atrophy (GA) progression in fields with and without pre-existing reticular macular disease (RMD) for 50 study eyes (P value = 0.0001, χ^2 test).

Total # of fields * with RMD	144	GA progressed	111
		No GA progression	33
Total # of fields without RMD	103	GA progressed	55
		No GA progression	48
Total # of fields ungradable for RMD	3	GA growth not calculated	
Total # of fields (50 study eyes × 5 fields/eye)	250	GA growth in RMD field	77.1% (111/144)
		GA growth in non-RMD field	53.4% (55/103)

* Fields = superior, inferior, temporal, and nasal quadrants, and central 3000- μ m-diameter circle.